Half the story: thermal effects on within-host infectious disease progression in a warming climate

Running head: Immunity in a warming climate

ALEXANDER STEWART[1], PASCAL I. HABLÜTZEL[2,3,4], MARTHA BROWN[2], HAYLEY V. WATSON[2,5], SOPHIE PARKER-NORMAN[2], ANYA V. TOBER[1], ANNA G. THOMASON[6], IDA M. FRIBERG[6], JOANNE CABLE[1§], JOSEPH A. JACKSON[6§*]

[1] *School of Biosciences, Cardiff University, Cardiff CF10 3AX, UK*

[2] *IBERS, Aberystwyth University, Aberystwyth SY23 3DA, UK*

[3] *Flanders Marine Institute, Oostende 8400, Belgium*

[4] *Laboratory of Biodiversity and Evolutionary Genomics, Biology Department, University of Leuven, 3000 Leuven, Belgium*

[5] *School of Environmental Sciences, University of Hull, Hull, HU6 7RX, UK*

[6] *School of Environment and Life Sciences, University of Salford, Salford M5 4WT, UK*

§ JC and JAJ are joint senior authors.

*Corresponding author: J.A.Jackson@Salford.ac.uk; tel. +44 161 2952240.

PRIMARY RESEARCH ARTICLE

29 **Abstract**

30 Immune defence is temperature-dependent in cold-blooded vertebrates (CBVs) and

31 thus directly impacted by global warming. We asked whether immunity and within-

32 host infectious disease progression are altered in CBVs under realistic climate

33 warming in a seasonal mid-latitude setting. Going further, we also asked how large

34 thermal effects are in relation to the effects of other environmental variation in such a

35 setting (critical to our ability to project infectious disease dynamics from thermal

36 relationships alone). We employed the three-spined stickleback and three

37 ecologically-relevant parasite infections as a "wild" model. To generate a realistic

38 climatic warming scenario we used naturalistic outdoors mesocosms with precise

39 temperature control. We also conducted laboratory experiments to estimate thermal

40 effects on immunity and within-host infectious disease progression under controlled

41 conditions. As experimental readouts we measured disease progression for the

42 parasites and expression in 14 immune-associated genes (providing insight into

43 immunophenotypic responses). Our mesocosm experiment demonstrated significant

44 perturbation due to modest warming (+2°C), altering the magnitude and phenology

45 of disease. Our laboratory experiments demonstrated substantial thermal effects.

46 Prevailing thermal effects were more important than lagged thermal effects and

47 disease progression increased or decreased in severity with increasing temperature

48 in an infection-specific way. Combining laboratory-determined thermal effects with

49 our mesocosm data, we used inverse modelling to partition seasonal variation in

50 *Saprolegnia* disease progression into a thermal effect and a latent

51 immunocompetence effect (driven by non-thermal environmental variation and

52 correlating with immune gene expression). The immunocompetence effect was large,

53 accounting for at least as much variation in *Saprolegnia* disease as the thermal

54 effect. This suggests that managers of CBV populations in variable environments

55 may not be able to reliably project infectious disease risk from thermal data alone.

56 Nevertheless, such projections would be improved by primarily considering

57 prevailing (not lagged) temperature variation and by incorporating validated

58 measures of individual immunocompetence.

59

60

Introduction

During infection, host immunity constrains the effectiveness with which a parasite exploits its host, determining disease outcome. In cold-blooded animals this within-host tension is modulated by environmental temperature, as both host immunity and parasite development are thermally dependent (Jackson & Tinsley, 2002; Garner *et al.*, 2011), each with a given thermal reaction norm (Scheiner, 1993). Where these reaction norms do not perfectly offset each other (Jackson & Tinsley, 2002), temperature changes, such as those generated during global warming, may shift susceptibility and disease progression within hosts. In turn, this may contribute to the wider dynamics of disease through changing the production rate of propagules (in definitive hosts) or the within-host survival of larval stages (in intermediate hosts). In natural environments, the size of thermal effects, and how these measure against the effects of non-thermal environmental variation (including variation driven indirectly by temperature regimen), is very poorly understood. Thus, it is equally poorly understood whether incremental warming would affect infectious disease systems mostly directly through thermal effects or indirectly through temperature-driven environmental variation. This dichotomy is key to our ability to project infectious disease dynamics on the basis of thermal relationships alone.

Given the above uncertainties, we set out to measure thermal effects on immunity and infectious disease progression in a cold-blooded vertebrate (CBV) model and to place these effects within the context of other natural environmental effects. We specifically focussed on within-host processes (excluding extra-host processes contributing to transmission) and considered a seasonal mid-latitude study system, which allowed the analytically powerful approach of using sinusoid functions to disentangle the contributions of distinct seasonally variable drivers. We created a realistic warming scenario, where we superimposed a thermal increment upon natural year-round environmental cycles, and observed the resulting variation. This allowed us to measure the perturbation caused by warming; but, critically, by itself did not allow us to quantify the separate thermal and non-thermal processes determining the observed outcomes. Crucially, we took the important further step of combining infection and thermal measurements from the realistic scenario with estimates from laboratory experiments where we had characterized thermal effects

94   precisely under controlled conditions. Taking a systems (inverse modelling) approach

95   we were then able to use sinusoid functions to analytically decompose the relative

96   contributions of thermal and non-thermal environmental effects.

97

98   We employed the mid-latitude three-spined stickleback (*Gasterosteus aculeatus*)

99   and its pathogens as a natural cold-blooded vertebrate (CBV) model. We kept in

100 mind that, in variable temperature regimens in natural habitats, past thermal variation

101 may feed forwards effects on physiological responses (Jackson & Tinsley, 2002;

102 Podrabsky & Somero, 2004; Raffel *et al.*, 2006, 2013, 2015; Garner *et al.*, 2011;

103 Murdock *et al.*, 2012; Dittmar *et al.*, 2014; Altman *et al.*, 2016). Our laboratory

104 experiments below therefore incorporated thermal change, allowing us to assess the

105 importance of both prevailing and time-lagged thermal effects on infectious disease

106 progression under natural seasonal thermal variation.

107

108 As phenotypic readouts we directly measured infection outcomes (Viney *et al.*, 2005)

109 in three ecologically-relevant infection systems with differing modes of established

110 infection. The directly-transmitted oomycete *Saprolegnia parasitica* (see Jiang *et al.*,

111 2013) produces a rapidly proliferating mould-like infection following initial

112 colonization by spores. Once established, these infections cause acute disease,

113 often overwhelming small fish hosts within hours or a few days post-infection. The

114 life history of the gyrodactylid monogenean *Gyrodactylus gasterostei* (see Harris,

115 1982), in contrast, is based on precocious (born near full size), directly-transmitted

116 viviparous flukes. A specialised larval transmission stage is absent: suprapopulations

117 persisting through *in situ* proliferation on individual hosts and the migration of

118 individuals from host to host. Gyrodactylid infections cause significant disease on

119 small fish that, if not fatal, may be self-limiting over a time scale of weeks or months.

120 In the cestode *Schistocephalus solidus* (see Barber & Scharsack, 2010) the

121 stickleback is the second intermediate host in an indirect life cycle, becoming

122 infected through the ingestion of copepod first intermediates. The non-proliferating *S.*

123 *solidus* plerocercoid larva may grow to great relative size (up to 50% of host weight,

124 or more), causing significant chronic disease and deformity over months or even

125 years. Our measurements for the respective infection systems (body surface

126 coverage by mycelia in *Saprolegnia*, abundance in *Gyrodactylus*, plerocercoid

127 weight in *Schistocephalus*) are in each case clear surrogates for disease

128   severity (Roberts, 2012). To provide insight into thermal effects on

129   immunocompetence we also measured (mRNA) expression for 14 immune-

130   associated genes representing different pathways (Hablützel *et al.*, 2016).

131

132   We quantified thermal effects under controlled conditions in two separate laboratory

133   experimental designs. These employed relatively large (but ecologically relevant)

134   temperature variations in order to increase the precision of estimated effects (i.e.,

135   maximizing the signal to noise ratio). One experiment examined the effects of

136   constant temperatures and of short-term temperature change, and the other the

137   effects of long-term cold exposures followed by periods of rising temperature

138   (simulating spring-like warming following winter). To generate the realistic warming

139   scenario mentioned above we conducted an outdoors mesocosm experiment using

140   an array of semi-natural tank habitats. We monitored phenotypes monthly, for a year

141   (from one autumn to the next), in a cohort of initially post-larval fish maintained in the

142   mesocosm tanks. The design was repeated twice, in separate successive years with

143   different fish cohorts. Half of the tanks were unheated and exposed to natural

144   temperature variation, whilst the other half were heated (precisely, using immersion

145   heaters with differential thermostatic control) to 2°C above the temperature of the

146   unheated tanks. This increment represents a large, but not unrealistic, stochastic

147   variation in mean temperature between successive years (O'Reilly *et al.*, 2015;

148   Sharma *et al.*, 2015) in temperate zone aquatic habitats. Such increases would be

149   expected to be more common, if as the Intergovernmental Panel on Climate Change

150   (IPCC) predicts, there is up to a 4.8°C rise in global mean surface temperature by

151   2100 (IPCC, 2014).

152

153   Our study aimed to represent processes in the field as far as possible whilst, at the

154   same time, exerting sufficient experimental control. Although, natural temperature

155   and photoperiod aside, tanks in our mesocosm experiment were not a fully natural

156   environment, they did undergo naturalistic cycles. Thus, seasonally variable

157   planktonic assemblages formed within the mesocosms and stickleback underwent

158   seasonal patterns of immune gene expression (Brown *et al.*, 2016), albeit that these

159   patterns were diminished from those seen in the wild (Hablützel *et al.*, 2016).

160   Furthermore, all of our experiments utilized quarantined anti-parasite treated wild fish

161   that had been acclimatized to laboratory or mesocosm conditions. In this choice of

162 hosts we aimed for subjects with as natural a phenotype as possible, but lacking

163 directly-transmitted pathogens capable of producing epidemics that might confound

164 the experimental structure. This approach was important given the likelihood that

165 laboratory-raised animals would have phenotypes very unrepresentative of the

166 wild (Robertson *et al.*, 2016).

167

168 Below we thus ask whether immunity and infectious disease progression in a model

169 naturally-occurring CBV are detectably perturbed in a realistic, seasonal, climate

170 warming scenario. We measure the size of thermal influences in the laboratory and

171 ask whether these are mediated by prevailing and lagged effects. Finally, combining

172 the different elements of our study (as outlined above), we partition thermal effects

173 on disease progression from effects due to other temporal environmental variation

174 and ask whether thermal effects are dominant in a natural seasonal environment.

175

176 **Materials and methods**

177 *Terminology*

178 For gene expression, we define prevailing thermal effects as those due to

179 temperature around the time of measurement and lagged effects as those due to

180 temperature at some interval before the time of measurement. For infections,

181 prevailing and lagged temperature effects are defined in relation to the timing of

182 parasite invasion. Prevailing thermal effects are those due to temperature within the

183 timeframe of infection. Lagged thermal effects are those due to temperature prior to

184 infection.
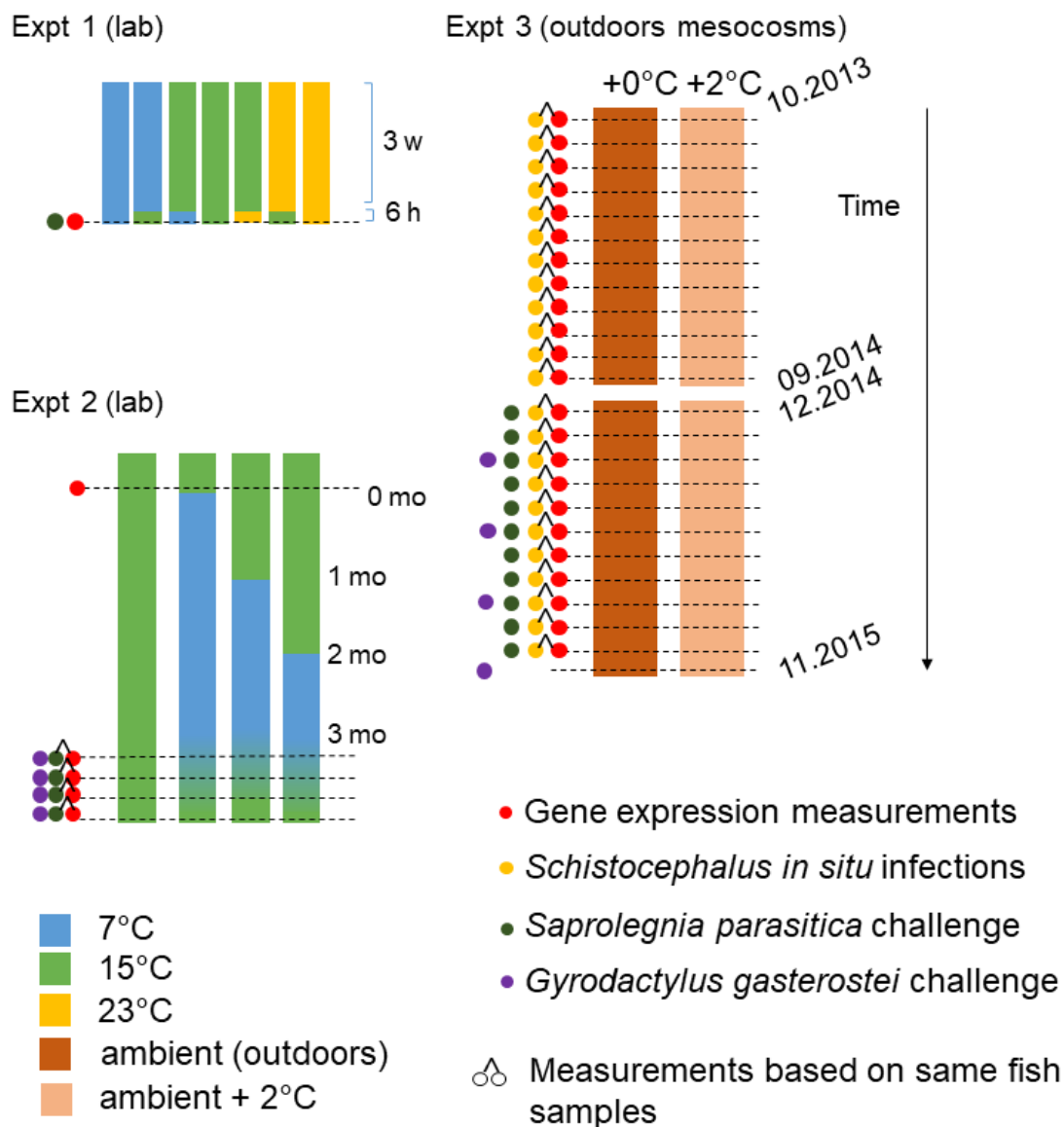
Fig. 1 Overview of experiments (expts) 1-3, showing timeline for temperature regimens (colour blocks), experimental time points (dotted lines) and experimental readouts associated with these points (circles). In the representation of experiment 2 the timings at the end of the experiment are not shown to exact scale for simplicity (precise timings are given in the materials and methods). For *Saprolegnia* and *Gyrodactylus* challenges, the time point shown is that for initial exposure. Abbreviations: h, hours; w, weeks, mo, months. Sample sizes within cells of these experiments are given in Tables S2-S4.

196 *Experimental designs and methods*

197 *Overview.* We carried out two laboratory experiments to characterize thermal effects

198 on infection and immunity under controlled conditions. Both of these featured

199 factorial combinations of prevailing and lagged temperature treatments. In the first

200 experiment (experiment 1) we subjected fish to different constant temperatures and

201 then to short-term temperature shifts. In the second (experiment 2) we subjected fish

202 to differing long-term cold temperature regimens (simulating winters of different

203 length) followed by synchronized convergence on a warmer temperature (simulating

204 spring-like warming). In a third experiment (experiment 3), to simulate climate

205 warming in a naturalistic seasonal environment, we maintained fish year-round in

206 semi-natural outdoor mesocosms, superimposing a small thermal increment upon

207 natural thermal variation. The structure of these experiments (involving experimental

208 manipulations of >1500 fish) is summarised in Fig. 1 and described in detail below

209 and in Supplementary appendix S1.

210 *Experiment 1 (prevailing temperature vs short-term lagged effects in the laboratory).*

211 Wild *G. aculeatus* captured at Roath Brook, Cardiff, Wales, U.K. (RBK; 51.4998°, -

212 3.1688°) in October 2014 and 2015 were transferred to the aquarium facility at

213 Cardiff University. Here they were quarantined at a density of <1 individual L^{-1} in 30 L

214 fresh water tanks at 15±0.5°C with 18L:6D photoperiod. All individuals were treated

215 for parasites using adaptations of treatments listed by Shinn & Bron (2012). Initially

216 fish were subjected to submersion in 0.004% formaldehyde solution for a total of 1 h

217 over a 1.5 h period (30 min exposure: 30 min rest in freshwater: 30 min exposure).

218 Following a further 24 h in fresh water, fish were then treated with praziquantel

219 (Vetark) according to the manufacturer's instructions (4 mg L^{-1} for 48 h). Following

220 this treatment, fish were maintained for 1 week in 1% aquarium salt solution and

221 0.002 g L^{-1} methylene blue to prevent secondary bacterial or fungal infection and

222 manually cleared of any remaining gyrodactylid infections following Schelkle *et al.*

223 (2009). Uninfected fish were then returned to fresh water (in 30L tanks, as above)

224 and acclimatised to laboratory conditions for a further one month quarantine period

225 (during which they were monitored for overt infections). Acclimatized fish were

226 weighed and measured (standardized body length, mm; body weight, mg) and

227 randomly allocated to 3 different groups (Fig. 1) that were respectively maintained at

228 7, 15 or 23°C for 3 weeks. Temperature treatment groups were then further sub-

229   divided (randomly) into temperature shift treatment groups. For the next 6 h these

230   temperature shift treatment groups were either maintained at the same temperature

231   as before (constant temperature groups), or shifted between temperatures (7 to

232   15°C, 23 to 15°C, 15 to 7°C and 15 to 23°C) (Fig. 1). Temperature treatments were

233   achieved within a suite of adjoining climate controlled rooms, in which temperature

234   varied ±0.5°C around the set temperature. After the 6 h temperature shift (lagged)

235   treatment, fish in all groups were subjected to *S. parasitica* exposure as described

236   below. Post-exposure, fish continued to be maintained at their final (prevailing)

237   temperature treatment until the sampling endpoint (72 h post-exposure). This

238   experiment was performed in eight time blocks (1-4 in 2014 and 5-8 in 2015); blocks

239   1-4 were excluded from analyses of infection outcome due to low overt symptom

240   rate. Fish from blocks 1-4 were processed for gene expression measurements.

241   Analyses of gene expression were thus based on blocks carried out in 2014 and

242   analyses of infection on blocks carried out in 2015. Final sample sizes entering

243   analyses (excluding losses due to technical failure) are broken down by experimental

244   cell in Table S2. All maintenance subsequent to the initial acclimation period and

245   before challenge exposure points was in 30 L fresh water tanks at a density of <1

246   individual L^{-1} and subject to a 18L:6D photoperiod. Fish were fed daily (*ad libitum*) on

247   chironomid larvae throughout the experiment.

248   *Experiment 2 (prevailing temperature vs long-term lagged effects in the laboratory).*

249   This experiment was carried out in two blocks separate in time: in the first of these *S.*

250   *parasitica* exposures were applied and in the other *G. gasterostei* exposures. Wild *G.*

251   *aculeatus* were captured at RBK in February 2014 (*Saprolegnia* block) and October

252   2014 (*Gyrodactylus* block). Treatment and acclimatization of fish prior to experiment

253   2 was as for experiment 1 (see above). Acclimatized fish were weighed and

254   measured (as above) and a random baseline sample preserved for gene expression

255   measurements. The remaining individuals were allocated to one of 4 long-term

256   temperature treatment (simulated winter length) groups. Over a total of 3 subsequent

257   months, these groups were first maintained at 15°C for 0, 1, 2 or 3 months and then,

258   respectively, at 7°C for 3, 2, 1 or 0 months (i.e., simulated winters of 0-3 months at

259   7°C with a synchronized end). Following this 3-month (lagged) treatment the group

260   already at 15°C continued to be maintained at this temperature, whilst those at 7°C

261   were raised to 15°C for the remainder of the experiment (Fig. 1). This 7-15°C

262 transition simulated an episode of rapid early spring warming and was carried out at

263 slightly different rates in the *Saprolegnia* and *Gyrodactylus* blocks (for operational

264 reasons). For the *Saprolegnia* block: temperature was raised at a rate of 1-2°C day^{-1}

265 over one week. For the *Gyrodactylus* block: temperature was raised at a rate of 0.5-

266 1°C day^{-1} over two weeks. Groups of fish from each of the simulated winter length

267 groups were subject to *S. parasitica* or *G. gasterostei* exposures (as described

268 below) at the end of the long-term temperature treatment, during the warming period,

269 and following the warming period. Average temperatures (prevailing temperature

270 treatments) on exposure days for the groups starting at 7°C were either 7, 7.5, 12.5

271 or 15°C for the *Saprolegnia* block and either 7, 9.5, 13 or 15 °C for the *Gyrodactylus*

272 block. Final sample sizes entering analyses are broken down by experimental cell in

273 Table S3. Post-exposure, fish continued to be subject to the wider experimental

274 thermal regimen (acclimation to 15°C and then subsequent maintenance at 15°C)

275 until the planned sampling endpoint. Other operational conditions were as described

276 for experiment 1.

277 *Experiment 3 (+2°C thermal manipulation superimposed upon natural environmental*

278 *cycles in outdoors mesocosms).* We utilized a system of outdoor mesocosms (12 ×

279 300 L recirculating tanks) at Aberystwyth University, U.K. equipped with precise

280 automatic temperature control and temperature monitoring. Six tanks were

281 unheated, whilst another 6 were thermostatically heated to 2.0326±0.0006°C above

282 ambient temperature (Fig. 2). Within this system we maintained separate *G.*

283 *aculeatus* year cohorts (see below) in 2013-2014 (October to September) and 2014-

284 2015 (December to November). Detailed technical specification of the recirculation,
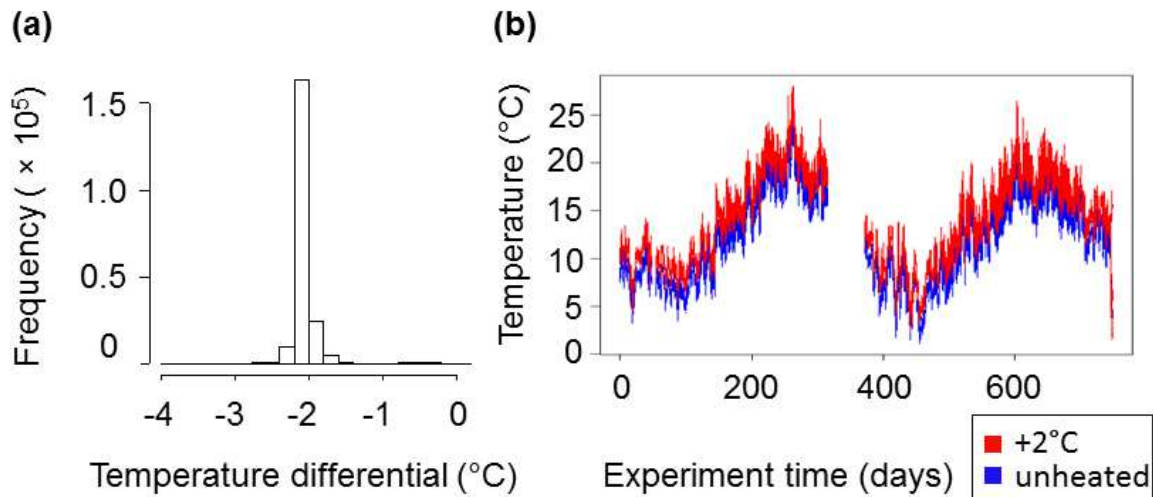
Fig. 2 Manipulation of temperature in mesocosm experiment (experiment 3). (a) Temperature differential between heated and unheated tanks based on 5-minutely recording (average temperature in heated tanks – average temperature in unheated tanks). (b) Temporal thermal variation in mesocosms: scatterplot of 5-minutely temperature recording for individual tanks. Experiment days are timed from November 4th 2013.

water quality management, environmental enrichment, temperature control and monitoring, stocking levels and sampling protocols are provided in Supplementary appendix S1. Briefly, fish were maintained at low biomass densities <0.05 g L^{-1}. They were fed daily with standard amounts of chironomid larvae, weekly supplemented with cladocerans. A small two-level manipulation of ration, orthogonal to the main explanatory variables of interest here, was carried out (by tank, in factorial combination with temperature treatment) as part of another study and a term for ration is included in statistical analyses below. For both iterations of the experiment post-larval young-of-the-year fish were captured in the wild at Llyn Frongoch (FRN; 52.3599,–3.8773), U.K., late in the breeding season, or after the end of the breeding season. To promote fish health during the subsequent experiment, all fish were subject to consecutive prophylactic anthelmintic praziquantel treatments (Hablützel *et al.*, 2016). Prior to the commencement of the experiment, fish were acclimatized for 4-6 weeks within the mesocosm system. Salinity was maintained throughout at 1% (10g L^{-1}) as a prophylactic measure to suppress opportunistic microbial

308   infections. Fish were sampled monthly from the mesocosm system for gene

309   expression measurements (October 2013 – September 2014; December 2014 –

310   October 2015). Ten individuals per month were taken from each thermal treatment

311   (1-2 individuals from each tank each month, in a sequence that approximately

312   equalized the number of fish taken from each tank in each quarter). These fish were

313   individually netted and immediately killed by concussion and then decerebration and

314   stored in RNA stabilization solution following Hablützel *et al.* (2016). Upon thawing

315   (prior to gene expression analysis, see below) they were dabbed dry, weighed and

316   measured (as above) and the abdominal cavity scanned for *Schistocephalus*

317   plerocercoids via a ventral incision. Total weight of any plerocercoid infection was

318   recorded and subtracted from the weight of the host. In the 2014-2015 experiment

319   run samples of fish were removed monthly (December 2014 - October 2015), for

320   exposure to *S. parasitica*, and separate samples of fish were removed quarterly

321   (February, May, August, November 2015), for exposure to *G. gasterostei*. These fish

322   were drawn in approximately equal numbers from the thermal treatments and

323   transported to Cardiff University for experimental infection procedures. Here, fish

324   were weighed and measured (as above) and maintained individually in 1L containers

325   exposed to ambient thermal variation in an outdoors facility. Salt concentration of the

326   water was reduced (from mesocosm levels) by 0.5% per day over two days, and

327   hosts were infected after a further day in fresh water (3 days after removal from the

328   mesocosm system). At Cardiff, all fish were fed daily, *ad libitum,* on chironomid

329   larvae and maintained under a single temperature regimen (outside ambient); any

330   effect of the mesocosm temperature treatment on infection outcome was thus a

331   lagged one. Final sample sizes entering analyses are broken down by experimental

332   cell in Table S4.

333   *Challenge infection protocols*

334   All experimentally challenged fish were maintained individually in standard 1 L

335   containers with 100% water changes every 48h and fed daily (*ad libitum*) on

336   chironomid larvae.

337   *Saprolegnia parasitica.* Isolate CBS223.65 of *S. parasitica*, derived in 1965 from

338   *Esox lucius* was used in challenge infections. Except in experiment 2 (see next), all

339   individual fish were subject to 30s ami-momi technique (Hatai & Hoshiai, 1993;

340   Stueland *et al.*, 2005) to increase permissiveness to infection and then either

341   exposed to 3×10^5 L^{-1} *S. parasitica* spore suspension for 24 h, or left non-exposed

342   but with otherwise identical maintenance conditions (control). For experiment 2 the

343   following exposure conditions were used: 1) no exposure (control); 2) ami-momi

344   treatment only; 3) exposure to *S. parasitica* spores following ami-momi treatment; 4)

345   exposure to *S. parasitica* spores without ami-momi treatment. Spore suspensions

346   prepared following Jiang *et al.* (2013) were generated independently for each

347   individual fish (or less frequently for pairs of fish) directly from a central stock of

348   CB223.65. At 72 h post-infection (p.i.) fish were individually netted and immediately

349   killed by concussion and then decerebration. (Extensive trials indicated that fish that

350   had not developed overt infection by 72 h p.i. did not subsequently develop

351   symptoms.) All specimens were rapidly weighed, measured (as above) and imaged

352   (in lateral view; digital Nikon S3600 camera) and then immediately preserved whole

353   in RNA stabilization solution (Hablützel *et al.*, 2016) for gene expression analysis.

354   Presence of *Schistocephalus* was determined via a ventral incision made to aid the

355   penetration of RNA stabilization solution (see Hablützel *et al.*, 2016). Using digital

356   images (above), the freehand selection tool in *ImageJ* (Abramoff *et al.*, 2004) was

357   employed to measure the overall surface area of the fish and the surface area

358   covered in erupted *S. parasitica* mycelia. Infection intensity was determined as the

359   proportional coverage.

360   *Gyrodactylus gasterostei.* An isogenic line of *G. gasterostei*, derived from a single

361   individual collected at RBK in October 2014 was used for experimental infections.

362   Identification was based on morphology (Harris, 1982) and genomic sequencing

363   (region: GenBank AJ001841.1) (Harris *et al.*, 1999). Fish were individually

364   anaesthetized in 0.02% MS222. Then, using a dissecting microscope and fibre-optic

365   lighting, the caudal fins of an infected donor and recipient fish were overlaid until 2

366   individuals of *G. gasterostei* transferred to the caudal fin of the recipient. Infected fish

367   were screened 24 h p.i. in fresh water under anaesthesia (0.02% MS222) and body

368   surfaces checked for infection; fish uninfected after this initial examination were re-

369   infected. Subsequently, fish were screened every 5 days for 91 days in experiment 2

370   and every 4-5 days for 58 days in experiment 3. At the experimental endpoints fish

371   were killed, weighed and measured (as above), and dissected to record parasites in

372   the body cavity, swim bladder, gut, gills and eyes (the only co-infecting parasite

373   recovered was *S. solidus*)*. G. gasterostei* is predominantly a parasite of external

374   body surfaces (>7000 fish examined from RBK have never contained this common

375   species in the branchial cavity; JC per. obs.).

376   *Thermal acclimation of parasites.* Source *Saprolegnia* and *Gyrodactylus* cultures

377   were maintained at a single intermediate temperature (15°C) prior to experiments to

378   provide infectious challenges with a standardized thermal reaction norm (given the

379   possibility of acclimation effects (Altman *et al.*, 2016)).

380   *Naturally-acquired infections persisting in experimental fish*

381   *Schistocephalus solidus* plerocercoid larva infections were refractory to the

382   prophylactic treatments described above and were the only naturally-acquired

383   macroparasite to carry over significantly into the experiments (*S.solidus* would have

384   been unable to transmit within experiments due to its indirect life cycle). Presence of

385   other macroparasites and overt microbial infections was confirmed to be at negligible

386   levels (<5% prevalence) through visual monitoring of experimental fish, direct

387   parasitological examination at endpoints (where sampling procedures allowed), and

388   by examination of animals prepared for, but unused in, experiments. The presence of

389   *S. solidus* infection was recorded in all experiments (see above) and included in

390   statistical analyses.

391   *Ethics*

392   Work involving animals conformed to U.K. Home Office (HO) regulations; elements

393   at Aberystwyth University were approved by the animal welfare committee of the

394   Institute of Biological, Environmental and Rural Sciences (IBERS), Aberystwyth

395   University and conducted in consultation with the HO inspectorate; elements at

396   Cardiff University were approved by the Cardiff University Ethics Committee and

397   conducted under HO licence PPL 302357.

398   *Gene expression measurements*

399   We measured expression of 14 immune-associated genes (Table 1) using

400   quantitative real-time PCR as previously described (Hablützel *et al.*, 2016). The

401   immunological roles of the genes are summarized in Table S1.

402

403   *Analyses*

404   All analyses were carried out in *R* version 3.2.3. In the statistical analysis of our

405   experimental results we employed linear mixed models (LMMs, package *lme4*) or

406   general linear models (LMs) for the confounder-adjusted analysis of gene expression

407   responses (the latter if no random term was significant). Power transformations

408   derived via a Box-Cox procedure were applied to individual expression variables on

409   a case-by-case basis following evaluation of standard model diagnostics. In a few

410   cases skewed gene expression variables containing some zeros were analysed in

411   generalised linear models for location, scale and shape (Rigby & Stasinopoulos,

412   2005, Stasinopoulos & Rigby, 2007) (GAMLSS) with a zero-adjusted gamma

413   distribution (using the package *gamlss*). For *Saprolegnia* infections we considered

414   the proportion of body surface coverage by erupted mycelia and analysed these data

415   in GAMLSS models. The latter employed a zero-inflated beta distribution

416   incorporating parameters for the probability (α) of not developing overt symptoms

417   (erupted mycelia) and also for the severity of symptoms (location parameter, μ,

418   reflecting coverage by mycelia in overt cases). For *Gyrodactylus* we considered

419   demographic parameters for continuously monitored individual infrapopulations (time

420   to peak infection and peak infection abundance) analysing these data in LMs with a

421   ($\log_{10}$ + 1) transformation. *Schistocephalus* infection data (total infection weight per

422   host, parasitic index [total infection weight / host weight]) were analysed in LMs, or in

423   generalized additive models (GAM) (Wood, 2006) when irregular trends were better

424   represented by non-parametric smoothers (package *mgcv*) (random intercept terms

425   for tank were not significant in these analyses). Except where otherwise stated,

426   statistical analyses of gene expression and infection metrics included explanatory

427   terms for the following in starting models: host length, sex, body condition (calculated

428   as residuals from a quadratic regression of weight on length), *Schistocephalus*

429   infection if this was present in the sample (present/absent; and except where this

430   infection was the analysed response), reproductive condition (breeding / non-

431   breeding condition; only in the long-term experiment 3), factorial experimental

432   treatments and experimental block (experiment 1) or year (experiment 3); sampling

433   (tank) and assaying (assay plate) structure was represented with random intercept

434   terms, where relevant. Interaction terms of interest were included where specified

435   below. The model for *Saprolegnia* infection in experiment 2 was developed using just

436 the thermal treatment terms and host terms significant in experiment 1, due to limited

437 sample size. Models for gene expression in experiments 1 and 2 included factors

438 representing exposure and overt infection with *Saprolegnia*; the experiment 2

439 analysis contained a fixed term for time (in degree days) within the experiment.

440 Random terms were assessed (in the full model) by likelihood ratio tests in LMMs

441 and GAMLSSs. When a random effect was added to a GAM as penalized regression

442 terms (to give a generalised additive mixed model, GAMM), its importance was

443 assessed by Akaike information criterion (AIC). Fixed model terms were retained

444 based on AIC for LMs, GAMLSSs and GAMs and *F*-tests (with Satterthwaite's

445 approximation to degrees of freedom) for LMMs. Reported *P* values were

446 determined by likelihood ratio tests in GAMLSSs, *F* tests in LMs, *F* tests with

447 Satterthwaite's approximation in LMMs and Wald tests in GAMs. Standard diagnostic

448 plots of residual and fitted values and quantile-quantile plots of residuals were

449 inspected for all models.

450 A sinusoid model (1) was employed to explicitly represent the possibility that the

451 direct thermal effect on resistance to *Saprolegnia* (α; probability of resisting overt

452 infection following exposure), as observed in laboratory experiments 1 and 2, was

453 counteracted by other seasonal environmental influences on host

454 immunocompetence in experiment 3:

455 *Saprolegnia* α = *x* + Immunocompetence driver (ID) + Thermal driver (TD)   (1)

456 $\text{ID} = c \times a \times \cos\left[\left(\frac{2\pi t}{12}\right) - \theta^1\right]$

457 $\text{TD} = d \times E$

458 $E = b \times \cos\left[\left(\frac{2\pi t}{12}\right) - \theta^2\right]$

459 Where E is environmental temperature (°C), *Saprolegnia* α is the monthly probability

460 of resisting overt *Saprolegnia* symptoms and *t* is time (months) (all observed in

461 experiment 3); parameters are detailed in Table 1. Given the seasonal nature of

462 temperature and *Saprolegnia α* variation in experiment 3, this model represents a

463 temperature driver (TD) and a putative immunocompetence driver (ID) with separate

464 (superimposed) annual sinusoid functions (Stolwijk *et al.*, 1999). We parameterized

465   the amplitude and acrophase of TD from our records of temperature (using

466   parameter estimates from cosinor regression of temperature against time, see

467   below) and the thermal coefficient, d (converting temperature into α, see Table 1),

468   from laboratory experiments (using an intermediate value based on analysis of

469   experiments 1 and 2). Taking an inverse modelling approach we then fitted this

470   partially parameterized model (1) to the monthly *Saprolegnia* α data (from

471   experiment 3) and estimated parameters associated with ID. For this we used

472   package *FME* (Soetaert & Petzoldt, 2010) to carry out constrained fitting of the

473   model. Cosinor regression (Tong, 1976) was carried out with package *cosinor* in

474   order to estimate the amplitude and acrophase of seasonal temperature variation.

475

476

Parameter	Definition	Estimate	Method of estimation
x	Constant	1.28 ± 0.37	Constrained fitting of *Saprolegnia* α data to (1)
c	Immunocompetence coefficient		
a	Amplitude of immunocompetence driver		
k	c × a	2.74 ± 0.53	Constrained fitting of *Saprolegnia* α data to (1)
Θ^1	Acrophase of immunocompetence driver	1.28 ± 0.29	Constrained fitting of *Saprolegnia* α data to (1)
d	Thermal coefficient	-0.375	Intermediate value from GAMLSS models (experiments 1 and 2)
b	Amplitude of thermal driver	5.02 ± 0.27	Cosinor regression of environmental temperature (E) on time (t)
Θ^2	Acrophase of thermal driver	1.30 ± 0.05	Cosinor regression of E on t

477

478

479   **Table 1** Parameters from sinusoid model of *Saprolegnia* α variation in experiment 3.

480

481   As descriptors of thermal variability in the 7-day windows preceding sampling points

482   in experiment 3 we considered temperature variance, amplitude of diel temperature

483   variation, the shape of the time series represented by Fourier coefficients, and the

484   maximum upward trend (given that in experiment 1 we observed a protective effect

485   of upward temperature shifts).To quantify diel temperature variation we fitted a GAM

486   to each time series, with parametric sinusoidal time terms to represent diel oscillation

487   and a non-parametric smoother for time to represent other temporal trends (Wood,

488   2006). Amplitude of the diel oscillation was calculated from the parameters of the

489   sinusoidal terms (Stolwijk *et al.*, 1999). Between-month distances based on Fourier

490   coefficients (FCD) were calculated from centred time series using package *TSdist*

491   (Mori *et al.*, 2017).

492

Results

The prevailing temperature consistently had substantial effects on infection and
immunity under controlled laboratory conditions

Both experiments 1 and 2 included factorial combinations of prevailing and lagged
thermal treatments. Considering the main effects of prevailing temperature first, we
found that most immune-associated genes (12/14) (Fig. 3a, Table 2; Fig. S2) showed
significant change in expression across the range 7-23°C (experiment 1) and many
(6/14) (Fig. 3a, Table 3; Fig. S3) did across the range 7-15°C (experiment 2). These
expression changes were consistent with monotonic responses (Fig. S2-S3). The
broad effect size of prevailing temperature on gene expression was substantial:
temperature variation across the range 7-23°C had a similar impact to sex and
greater impact than other host variables such as size, body condition and infection
status (Fig. S4).

Gene	Model type	T (7-23°C)		Δ T (-8, 0, +8°C shift)	
		Parameter	*P*	Parameter	*P*
cd8a	LM	0.009±0.001	1.7×10^{-8}		
ighm	LM	0.007±0.001	5.5×10^{-11}	-0.004±0.001	4.0×10^{-5}
ighz	GAMLSS	α -0.096±0.045	0.028	α 0.012±0.050	0.009
foxp3b	LM	0.009±0.002	9.6×10^{-6}	-0.006±0.002	0.009
il4	LMM	0.0004±0.0002	0.037		
il17	LMM	-0.002±0.001	0.035		
orai1	LMM	-0.003±0.001	2.5×10^{-5}		
tirap	LM	0.009±0.001	5.7×10^{-13}		
tbk1	LMM	-0.0014±0.0002	2.8×10^{-12}		
il1r1	LMM	0.005±0.002	0.004	-0.005±0.002	0.010
lyz	LM	0.010±0.002	2.1×10^{-6}		
defbl2	LM	0.008±0.002	2.4×10^{-4}		

Table 2 Significant effects of thermal regimen on immune gene expression in
experiment 1. Parameters and *P* values for prevailing temperature (T) and prior
thermal shift (ΔT). T and ΔT are represented as continuous variables; no additional
genes were found to be thermally-dependent through representing T and ΔT with
quadratic terms. Data were analyzed in confounder-adjusted general linear models
(LM), linear mixed models (LMM) and generalized additive models for location, scale

514 and shape (GAMLSS). Genes without significant effects for T or ΔT are omitted;

515 there were no significant T × ΔT effects. Note that for the GAMLSS model above the

516 parameter sign is opposite to the direction of the biological effect.

517

Gene	Model type	T (7-15°C)		WL (0-3 months at 7°C)	
		Parameter	*P*	Parameter	term *P*
ighm	LMM			1 mo -0.012±0.006 2 mo -0.019±0.006 3 mo -0.016±0.007	0.013
il17	LM	-0.005±0.003	0.090	3 mo 0.077±0.027	0.020
il12ba	LM	0.019±0.007	0.005		
orai1	LM	-0.015±0.004	0.001		
tbk1	LMM	-0.010±0.002	9.1×10^{-6}		
il1r1	LMM			2 mo 0.014±0.007 3 mo 0.028±0.008	0.002
defbl2	LM	0.016±0.005	0.002		
gpx4a	LMM	-0.0007±0.0002	1.8×10^{-3}	1 mo 0.0035±0.0018 2 mo 0.0061±0.0019 3 mo 0.0056±0.0020	0.011

518

519

520 **Table 3** Significant effects of thermal regimen on immune gene expression in

521 experiment 2. Parameters and *P* values for prevailing temperature (T) and simulated

522 prior winter length (WL). T is represented as a continuous variable (no additional

523 genes were found to be dependent on T through adding a quadratic term); WL is

524 represented as a factor as differences were associated with any simulated winter

525 exposure or only with longer exposures. Data were analyzed in confounder-adjusted

526 general linear models (LM), linear mixed models (LMM) and generalized additive

527 models for location, scale and shape (GAMLSS). Genes without significant effects

528 for T or WL are omitted; there were no significant T × WL effects.

529

530 In *Saprolegnia* challenges (Fig. 3b-c), resistance to overt disease (α parameter)

531 became less probable with increasing prevailing temperature in both laboratory

532 experiments (GAMLSS analyses; experiment 1, α = -0.12±0.04, *P* = 2.9×10^{-3},

533 experiment 2, α = -1.05±0.46, *P* = 1.1×10^{-5}). In *Gyrodactylus* challenges in

534 experiment 2, low temperature exposure during the early stages of established

infection produced a more severe outcome: parasite abundance peaking later and higher (Fig. 3f, g) (LMs; $\log_{10}$ time to peak = -0.04±0.01, P = 6.1 × 10^{-3}; $\log_{10}$ peak population = -0.07±0.02, P = 9.5 × 10^{-4}). Notably, data presented by Harris (1982) indicate that *G. gasterostei* infrapopulations also peak later and higher when maintained at a constant temperature of 10 compared to 15°C. The direction of these thermal effects on peak parasite numbers is contrary to the expectation that such a temperature increase would promote *Gyrodactylus* population growth in permissive conditions (Harris, 1982; Gelnar, 1990; Jackson & Tinsley, 1994; Sereno-Uribe *et al.*, 2012), and indicative that low temperature impairs the early development of resistance responses (Andersen & Buchmann, 1998).
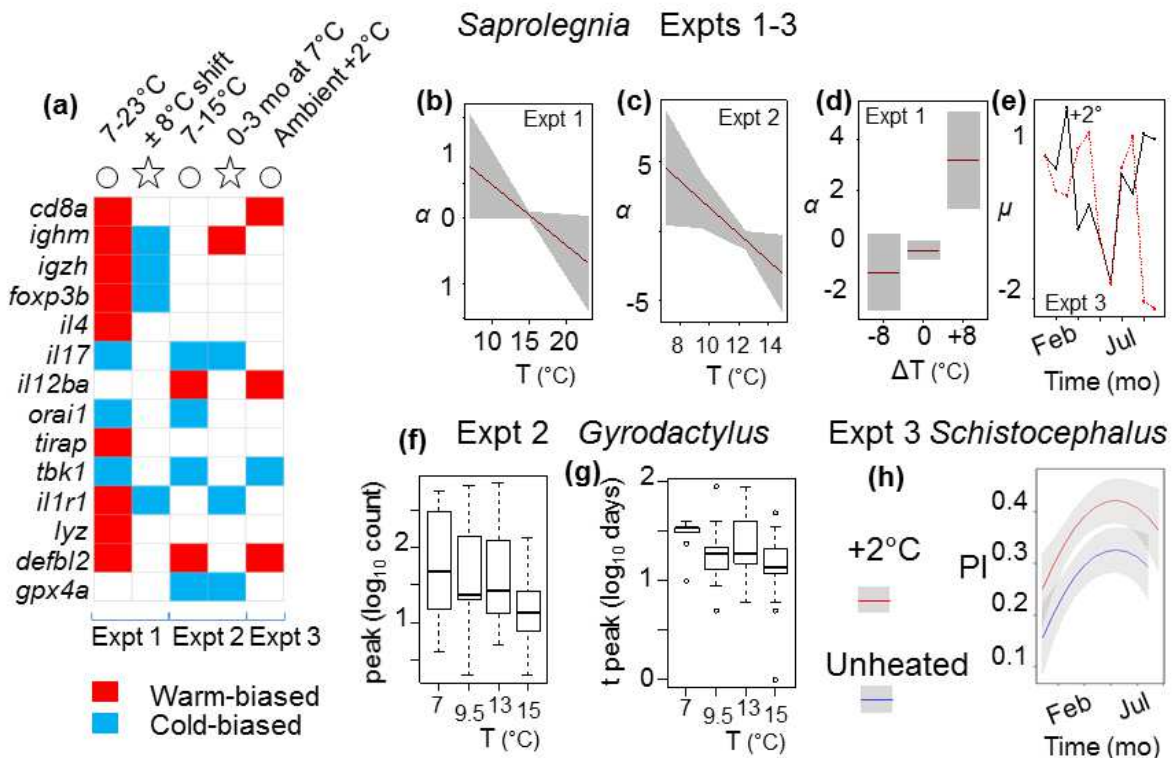
Fig. 3 Effects of prevailing temperature and past temperature change on gene expression and disease progression in experiments. (a) Colour matrix showing

553   significant gene expression responses to temperature regimens in experiments 1, 2

554   and 3 (see key). Open circles indicate responses to prevailing temperature and stars

555   responses to previously experienced temperature change (i.e., lagged effects). As

556   expected, the numbers of genes responding detectably to prevailing temperature fell

557   with the thermal range examined in the respective experiments (experiment 1, 16°C

558   range: 12/14 responsive genes; experiment 2, 8°C range: 6/14 responsive genes;

559   experiment 3, 2°C range: 4/14 responsive genes). There was consistency across

560   experiments in the sign of significant responses to prevailing temperature, which

561   were always the same for a given gene (10 comparisons). Fewer genes (< half the

562   number) responded detectably to lagged temperature effects than to prevailing

563   temperature across experiments 1 and 2. For lagged effects shown in (a), genes are

564   termed cold-biased if they had higher expression than expected following a

565   downwards temperature shift (experiment 1) or if they responded positively to

566   increasing winter length (experiment 2). (b-e) Significant responses of *Saprolegnia*

567   infection outcome to thermal regimen in experiments 1-3; plots (on the scale of the

568   model linear predictor) show confounder-adjusted effects from generalized additive

569   models for location, scale and shape (GAMLSS) with 95% confidence intervals

570   (shaded). In experiments 1 (b) and 2 (c) the probability of not developing overt

571   symptoms (α) decreased with increasing prevailing temperature. There was a

572   protective residual effect of a recent +8°C temperature shift in experiment 1 (d). In

573   experiment 3 symptom severity (μ) was subject to a time × temperature treatment

574   (+2°C) interaction (e). (f-g) Significant responses of *Gyrodactylus* infrapopulation

575   dynamics in experiment 2. Lower initial exposure temperature (shown on the x –

576   axis) resulted in infections with higher (f) and later (g) abundance peaks (*peak*,

577   highest count; *t peak*, time to reach highest count). Box-and-whisker plots show log-

578   transformed data for individual infrapopulations (only exposure temperature was

579   significant in statistical models). (h) Response of *Schistocephalus* parasitic index

580   (infection weight / host weight, PI) to a +2°C manipulation across the year in

581   experiment 3 (outside mesocosms). PI was significantly greater in hosts from heated

582   mesocosms. Lines are confounder-adjusted effects from a general linear model (LM)

583   with 95% intervals (shaded).

584

585   *Lagged effects of past temperature on infection and immunity were detectable but*

586   *not consistently important*

587   Some main effects of lagged thermal treatments were evident in the gene expression

588   results in both laboratory experiments (Fig. 3a, Tables 2-3). However, lagged thermal

589   effects occurred much less frequently (Fig. 3a) than prevailing temperature effects

590   (14 genes showed significant prevailing effects and 6 genes significant lagged

591   effects in one or both of experiment 1 and 2). There were no effects on gene

592   expression due to interactions between prevailing temperature and preceding

593   temperature treatments in either experiment.

594

595   There were no lagged main effects of temperature on *Saprolegnia* infections in

596   experiments 1 or 2. This was with the exception of a single scenario: where rapid

597   upward shifts in temperature in experiment 1 had a protective effect (increasing α)

598   (Fig. 3d) (GAMLSS analysis; +8°C shift α = 3.92±1.20, reference level = -8°C shift;

599   term deletion P = 1.1 × 10^{-4}). For *Gyrodactylus* in experiment 2 we found no effect of

600   past temperatures previous to the period of infection (i.e., of simulated winter length)

601   on infrapopulation dynamics. No interactions occurred between lagged temperature

602   and prevailing temperature treatments for *Saprolenia* (experiments 1-2) or

603   *Gyrodactylus* (experiment 2).

604   *Thermal effects on infection and immunity were readily detectable in a realistic*

605   *warming scenario superimposed upon natural environmental cycles*

606   Turning to our mesocosm experiment we first asked what effect the +2°C

607   manipulation (simulating climate warming) had on gene expression and infection

608   outcomes. We found that several genes responded significantly (*cd8a*, *il12ba*,

609   *defbl2*, *tbk1*; always in the same direction as responses in laboratory experiments),

610   even against the background of natural seasonal variation (Fig. 3a; Table 4). For

611   *Schistocephalus* infections *in situ* within the mesocosms, the direct effect of the +2°C

612   increment increased the parasitic index (infection weight/host weight, PI) (Fig. 3h)

613   (LM; +2°C 0.095±0.023, P = 1.1 × 10^{-4}) and plateroceroid weight (GAM; +2°C

614   10.9±4.6, P = 0.02) although without the extreme plerocercoid size increases

615   reported in recent constant temperature experiments (Macnab & Barber, 2012).

616   There was no lagged main effect of the +2°C temperature manipulation on

617   *Saprolegnia* and *Gyrodactylus* infection outcomes in fish extracted from the

618   mesocosms and equalized to the same (natural) temperature regimen before

619   exposure to infection. However, there was a significant month × lagged temperature

620   treatment interaction for symptom severity in *Saprolegnia* (*μ* parameter), with

621   modulated infection outcomes in the winter and late summer (Fig. 3e) (GAMLSS;

622   +2°C × month: Feb^{low} -1.69±0.81, Aug^{low} 2.400±1.16, Sept^{low} -3.90±1.15; term

623   deletion *P* = 7.9 × 10^{-4}).

624

Gene	Model type	Parameter (+2°C)	*P*
cd8a	LMM	0.0248±0.0122	0.042
il12ba	LM	0.0804±0.0209	1.7 × 10^{-4}
tbk1	LMM	-0.0713±0.0194	2.7 × 10^{-4}
defbl2	LMM	0.0012±0.0003	4.2 × 10^{-5}

625

626   **Table 4** Significant effects of thermal regimen on immune gene expression in

627   experiment 3. Parameters and *P* values for thermal treatment (unheated / +2°C).

628   Data were analyzed in confounder-adjusted general linear models (LM), linear mixed

629   models (LMM) and generalized additive models for location, scale and shape

630   (GAMLSS). Genes without significant effects for thermal treatment are omitted.

631   *Given thermal responses observed in the laboratory, disease progression was*

632   *paradoxically highest in winter in an environment with natural seasonality*

633   We next asked how well the year-round patterns of infection susceptibility seen in

634   mesocosms (experiment 3) corresponded to the observed responses in our

635   laboratory manipulations of temperature. In the more realistic mesocosm setting

636   there was striking evidence that seasonal trends were superimposed upon direct

637   thermal effects, leading to results unpredictable on the basis of thermal variation

638   alone (Zimmerman *et al.*, 2010). Thus, the probability of resisting overt *Saprolegnia*

639   infection (α parameter), which decreased when temperature was increased in the

640   laboratory (Fig. 3b, c), paradoxically was lowest during winter in the mesocosms

641   (Fig. 4a) (GAMLSS; α Feb - 2.49±0.79; month term deletion, *P* = 1.8 × 10^{-4}). A

642   corresponding pattern was seen in *in situ Schistocephalus* infections in the

643   mesocosms. As described above (see also Fig. 3h), the +2°C temperature
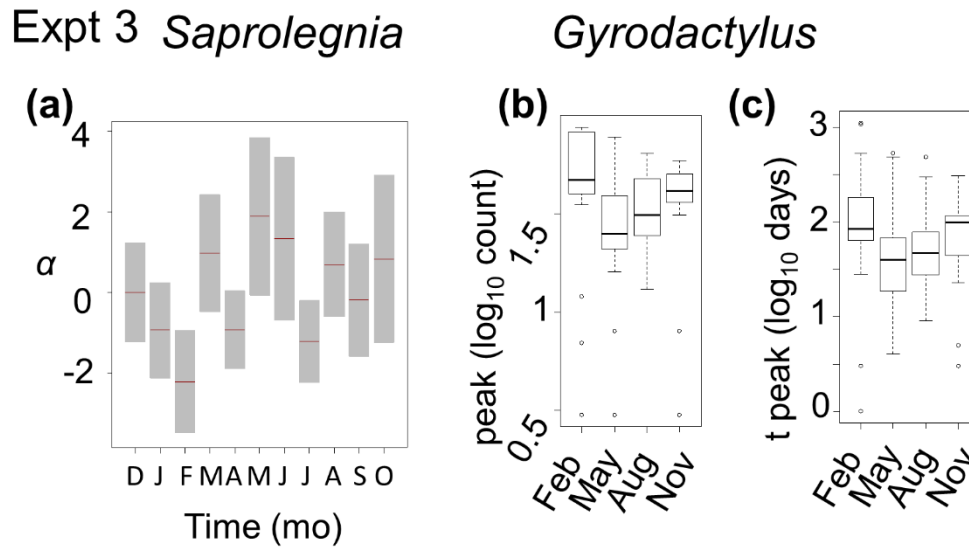
Fig. 4 Greater disease progression (following challenge infections) in winter in an outdoors seasonal environment (experiment 3). (a) For *Saprolegnia*, probability of not developing overt symptoms (*α*) was significantly variable in time and lowest in February; plot shows confounder-adjusted effects from a generalized additive model for location, scale and shape (GAMLSS) with 95% confidence intervals shaded (on the scale of the model predictor). (b-c) *Gyrodactylus* infrapopulations monitored through winter months (starting in November or February, compared to May or August) had higher (b) and later (c) abundance peaks (*peak*, highest count; *t peak*, time to reach highest count). Box-and-whisker plots show log-transformed data for individual infrapopulations (only exposure month was significant in statistical models).

manipulation produced an increase in PI, indicating a positive thermal dependence of disease severity (as for *Saprolegnia* α). Contrary to this thermophilic trend, though, PI in fact increased during the winter months (Fig. 3h) and ceased to increase thereafter (LM with quadratic term for time; time 0.056±0.015, $P = 0.014$; time^2 -0.004±0.001, $P = 2.7 \times 10^{-3}$). This pattern is consistent with lowered host resistance during winter and rapid plerocercoid growth (relative to the host) despite low winter temperatures. For both *Saprolegnia* and *Schistocephalus*, the pattern of results is thus suggestive of a seasonal immunocompetence variable (low host immunocompetence in winter) that acts in opposition to the direct effects of

666   prevailing environmental temperature (positive thermal dependence of host

667   exploitation, as demonstrated in experiments 1 and 2). For *Gyrodactylus,* as for

668   *Saprolegnia* and *Schistocephalus*, the worst disease also occurred in winter (Fig. 4b,

669   c), with infection abundance peaking later (LM; $\log_{10}$ time to peak, Aug 0.14±0.09,

670   Nov 0.21±0.08, Feb 0.30±0.077, reference May; month term deletion $P = 9 \times 10^{-4}$)

671   and higher (LM; $\log_{10}$ peak population; Aug 0.17±0.15, Nov 0.32±0.14, Feb

672   0.43±0.12; $P = 0.007$).

673   *A latent seasonal immunocompetence variable, that correlated with immune gene*

674   *expression and opposed thermal effects, explained winter-biased disease*

675   *progression in natural circumstances*

676   We set out to explicitly partition seasonal thermal and immunocompetence effects

677   contributing to the winter-biased pattern of infection susceptibility seen in experiment

678   3. We focussed on *Saprolegnia*, for which most experimental data were available

679   and for which the binary infection endpoint (α) simplified interpretation. As seasonal

680   fluctuation can be represented with sinusoid functions (Stolwijk *et al.*, 1999), we

681   constructed a model explaining the (logit scale) *Saprolegnia* α parameter in terms of

682   a cosine wave for annual thermal variation and another cosine wave for seasonally-

683   varying immunocompetence (see (1), Table 1, Fig. 5). We first parameterized the

684   amplitude and acrophase of the annual temperature function from our 2014-2015

685   temperature monitoring data and estimated the coefficient converting this into

686   infection rate from observations on the effect of prevailing temperature in

687   experiments 1 and 2. (We did not include lagged thermal effects because of the lack

688   of these in experiments 1 and 2, except for the protective effect of previous sharp

689   warming; although we do examine the latter, and other aspects of thermal variance,

690   further below.) We then used an inverse modelling approach to compute the

691   parameters of the latent immunocompetence function by fitting the partially

692   parameterized model to our 2014-2015 *Saprolegnia* infection data. The fully

693   parameterized model explained 22% of the variation in *Saprolegnia* α, and

694   suggested that effects driven by temperature and by seasonal immunocompetence

695   were almost collinear (Fig. 5). Importantly, we note that the distinct contributions of

696   temperature and immunocompetence would therefore have been unobservable had

697   only infection data been available (as in many field studies).

698

699
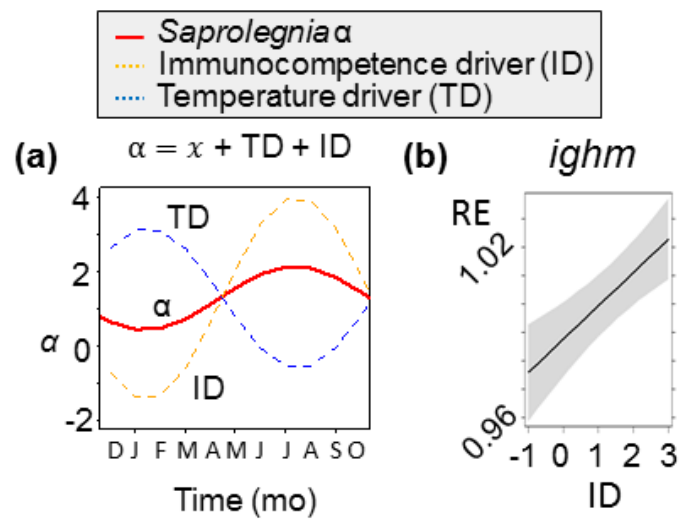
Fig. 5 A latent immunocompetence variable, which independently correlates with seasonal expression in immunity genes, reconciles observations from laboratory and outdoors mesocosm experiments. (a) Results of an inverse model of observed variation in *Saprolegnia* α in experiment 3: α is explained via the superimposition of a sinusoidal seasonal temperature driver, TD (parameterized from observed relationships with temperature in the laboratory and from field temperature records), and a hypothetical (latent) sinusoidal immunocompetence variable, ID (parameterized by constrained fitting of α data to the model); x is a constant. (b) The association of the latent immunocompetence variable from the analysis shown in (a) with *ighm* relative expression (RE) in experiment 3; line shows confounder-adjusted effect (on the scale of the model linear predictor) from a linear mixed model (LMM) with random intercepts for month; 95% confidence interval shaded.

712

We considered whether the latent immunocompetence variable derived above might represent the protective lagged effect of sharp temperature rises, as observed in experiment 1, or of other aspects of preceding temperature variability, but found this to be unlikely. As immunocompetence and prevailing temperature were collinear (see above), we expected that any component of temperature variability predominantly driving immunocompetence would necessarily be correlated with

719　prevailing temperature. Therefore, we examined different descriptors of temperature

720　variability (in the week before monthly sample points) for this correlation.

721
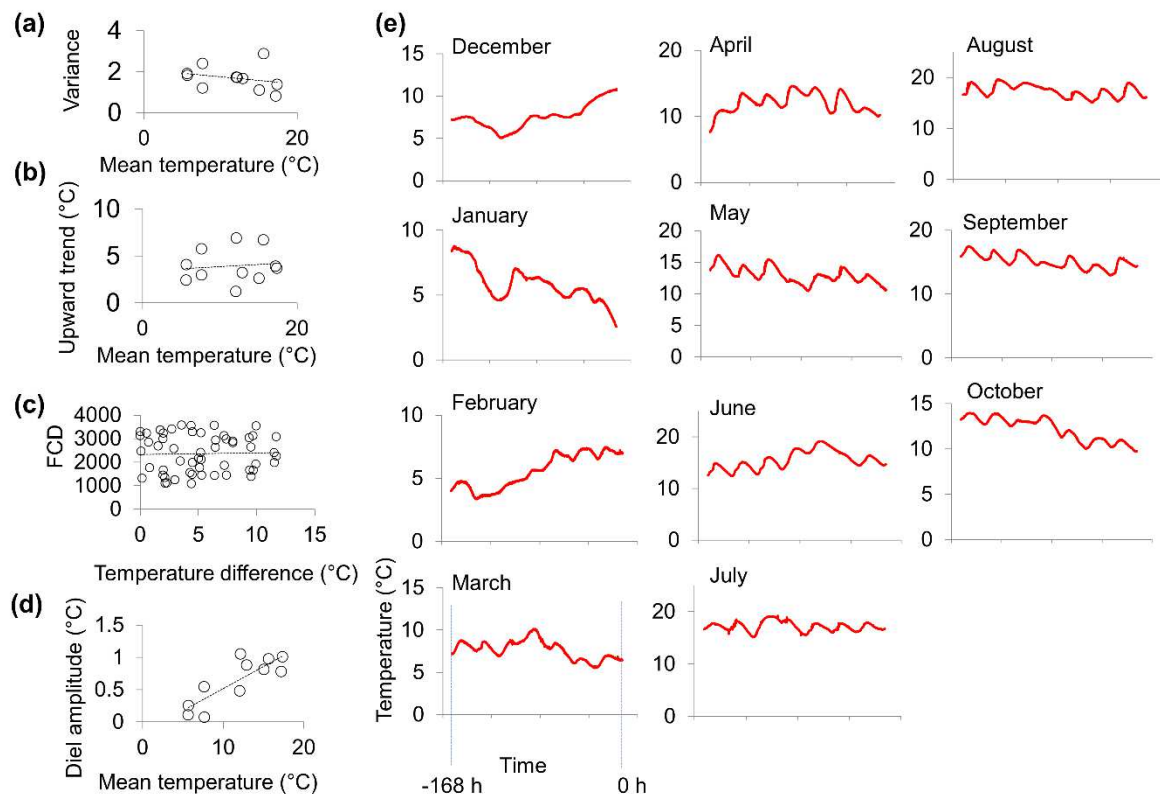
722

723　**Fig. 6** Association between descriptors of temperature variability and mean

724　temperature in outdoors mesocosms. (a) variance vs mean temperature; (b)

725　maximum upward trend vs mean temperature; (c) pairwise month-to-month

726　distances between time series shapes (Fourier coefficient distances, FCDs) vs

727　pairwise month-to-month temperature differences; (d) amplitude of diel temperature

728　variation vs mean temperature. Analyses shown above are based on the final 7-day

729　period fish spent in the mesocosm habitats prior to monthly exposures to

730　*Saprolegnia* in the 2014-2015 run of experiment 3. Panel (e) shows monthly

731　temperature trajectories for the 7-day period analyzed, from -168 to 0 h.

732

733　The maximum upward trend, variance and shape (FCD) of monthly temperature time

734　series (in the week before sampling) were not associated with mean monthly

735   prevailing temperature (Fig. 6a-c). Although the amplitude of diel temperature

736   variation did increase with temperature (Fig. 6d), the absolute size of this increase

737   was small (~ 1°C across the annual thermal range; corresponding to a ~ 2°C diel

738   range difference) when considered in the light of the effect size for a +8°C shift on

739   *Saprolegnia* α in experiment 1. The latter corresponded to a change in α of 0.8

740   across 2°C (the annual diel range difference), compared to an annual α range of >5

741   for the immunocompetence driver shown in Fig. 5a.

742   We also asked whether the latent immunocompetence variable was associated with

743   independent data for the expression of immunity genes. We found that one gene,

744   *ighm* (P = 0.003) (Fig. 5b), was clearly associated and that four others were more

745   marginally associated: *il4* (P = 0.07), *tirap* (P = 0.04), *defbl2* (P = 0.06) and *cd8a* (P

746   = 0.06) (in confounder-adjusted LMMs, with random intercepts for month). In all of

747   these cases, increased expression corresponded to increased latent

748   immunocompetence. The association with *ighm* is consistent with the suspected

749   involvement of antibodies in resistance to *Saprolegnia* infection (Minor *et al.*, 2014)

750   and with elevated early autumn anti-*Saprolegnia* antibody seropositivity in wild

751   salmonids (Fregeneda-Grandes *et al.*, 2009).

752

753   **Discussion**

754   We focussed on the three-spined stickleback and its pathogens as a natural

755   experimental model. We readily detected perturbation of immune expression and

756   infectious disease progression in a realistic experimental climate warming scenario

757   applied in naturalistic outdoors mesocosms. Even for a modest thermal increment

758   (+2°C), significant expression differences were observed for 4/14 immune-

759   associated genes examined (*cd8a*, *tbk1*, *il12ba*, *defbl2*) whilst *Schistocephalus*

760   parasitic index and plerocercoid growth increased. Lagged thermal effects on

761   *Saprolegnia* symptom severity (μ) also featured in a significant interaction with

762   month. This interaction reflected a distinctive seasonal pattern of disease

763   progression in the warmed environment, demonstrating the potential for change in

764   the phenology of disease (Buehler *et al.*, 2008; Paull & Johnson, 2014) under

765   climate warming.

766   In CBVs like the three-spined stickleback, within-host infection dynamics can thus be

767   expected to respond appreciably to rapid year-on-year warming. Direct thermal

768   effects may drive part of this response, which in turn contributes to

769   population- (Barber *et al.*, 2016; Mignatti *et al.*, 2016) and community-

770   level (Karvonen *et al.*, 2013; Paull & Johnson, 2014) pathogen dynamics. But these

771   higher-level responses will also depend on other factors: on thermal responses of

772   free-living transmission stages and on indirect effects of temperature (on both within-

773   host and free-living stages) mediated through changes in the environment. It is

774   important (as we describe below in the case of thermal and non-thermal

775   environmental influences on *Saprolegnia* disease progression) to decompose such

776   complex composite processes into their fundamental parts, if we are to understand

777   the sources of dynamical change in natural systems.

778   To estimate thermal effects (holding other environmental effects constant) we carried

779   out laboratory experiments with factorial combinations of lagged and prevailing

780   temperature treatments. The controlled conditions in these experiments would have

781   prevented the formation of seasonal environmental variation (e.g., plankton

782   development) as occurred in the mesocosm experiment. The laboratory

783   experiments, together with the mesocosm experiment (above), not unexpectedly (Bly

784   & Clem, 1992; Maniero & Carey, 1997; Le Morvan *et al.*, 1998; Makrinos & Bowden,

785   2016) confirmed a major general effect of temperature in modulating immunity and

786   within-host infectious disease outcomes in CBVs. All of the 14 gene expression

787   measures and all 3 infection systems that we examined showed some significant

788   response to experimental manipulation of temperature, in many cases with

789   substantial effect sizes. Whilst other studies of ectothermic organisms have

790   emphasized the importance of lagged thermal influences on immunity, we found that

791   thermal effects were mediated most powerfully by the prevailing temperature.

792   Overall, less than half the number of genes (in experiments 1 and 2) showed

793   expression responses to past thermal variation as to prevailing temperature. All three

794   of our infection systems showed the effect of temperature prevailing within the

795   timeframe of infection, but there were few cases in which temperature prior to this

796   timeframe was important. Amongst the lagged thermal treatments in our laboratory

797   experiments only sharp temperature rises had any significant effect: decreasing the

798   probability of developing of overt *Saprolegnia* infection. As discussed above, there

799   was also an interaction between lagged thermal treatment and *Saprolenia* symptom

800   severity (μ) in the mesocosm experiment. Putting these results in perspective, we

801   note that the lagged temperature treatments we used in laboratory experiments

802   (simulated winters 0-3 months long and 8°C thermal shifts over 6 h) were relatively

803   extreme. This would have exaggerated the importance of lagged compared to

804   prevailing temperature effects, as the latter were represented in our experiments by

805   a set of values well within the natural range. Interestingly we did not find an anti-

806   protective effect of sharp temperature falls on *Saprolegnia* infection. Whilst such a

807   tendency has been reported in saprolegniosis of channel catfish (Bly *et al.*, 1992),

808   and in fungal infections of lower vertebrates (Raffel *et al.*, 2013), our results suggest

809   this effect is not a general one. Even leaving the effects of the non-thermal variation

810   (see below) aside, our data indicate that past temperature records will be of limited

811   use for managers of CBV populations in projecting infectious disease susceptibility.

812   Rather systems for the projection of disease risk based on prevailing temperature

813   variation will be more effective.

814

815   Combining our mesocosm and laboratory experimental data we considered the

816   contributions of thermal and non-thermal environmental variation to disease

817   progression. Importantly, in the outdoors mesocosm environment (subject to biotic

818   and abiotic seasonality), *Saprolegnia* and *Schistocephalus* infections occurred in a

819   pattern not explained by their responses to experimental thermal manipulations. In

820   both infections disease progression was increased by upwards experimental

821   manipulation of temperature, all other things being equal, but under mesocosm

822   conditions was also at its greatest in winter. Crucially, our study design allowed us to

823   partition thermal effects from other environmental effects on disease progression,

824   revealing their relative magnitude. Using an inverse modelling approach to represent

825   monthly *Saprolegnia* challenge infection outcomes in the outdoor mesocosms, and

826   including (prevailing) thermal effects parameterized from our laboratory experiments,

827   we were able to derive a seasonal latent variable opposing (and slightly

828   outbalancing) thermal effects. This variable represented environmental effects on

829   anti-*Saprolegnia* immunocompetence, other than those due to the prevailing

830   temperature, and reconciled laboratory and mesocosm observations. It could not be

831   explained by seasonal patterns of temperature variance (cross-referencing to effects

832   observed in laboratory experiments), and was independently (positively) correlated

833   with monthly expression of the immunoglobulin M heavy chain gene *ighm*. This is of

834   note because of the likely relevance of IgM for resistance to *Saprolegnia* (Minor *et*

835   *al.*, 2014). Furthermore, as teleost IgM antibodies may have a short half-life (1-3

836   days) (Voss Jr *et al.*, 1980; Ye *et al.*, 2010, 2013), a link between levels of heavy

837   chain mRNA and functional antibody is not unrealistic.

838   Thus, the non-thermal environmental contribution (via seasonal immunocompetence

839   effects) to *Saprolegnia* disease progression variance is large (of similar size to the

840   thermal contribution, slightly outbalancing it across the year). Whilst it is beyond the

841   scope of the present study to determine the environmental agents involved, such

842   seasonal variation in immunity is well known in other vertebrate systems

843   (Beldomenico *et al.*, 2008; Martin *et al.*, 2008). It should be pointed out, moreover,

844   that although some seasonal variation in the expression of immunity genes occurs in

845   mesocosm fish, we have previously observed such responses to be diminished

846   compared to those in the wild (Hablützel *et al.*, 2016). This suggests that the

847   component of disease progression variation determined by non-thermal

848   environmental effects on immunocompetence, and not directly by temperature, may

849   be even larger under fully natural conditions in the wild.

850

851   We note, additionally, the variable sign in the disease responses of our 3 infection

852   systems to prevailing temperature manipulations (positive for *Saprolegnia* α and

853   *Schistocephalus* parasitic index and negative for *Gyrodactylus* abundance). This is

854   consistent with the simple theoretical scenario, introduced at the beginning, where

855   disease worsens or ameliorates determined by the interplay of species-specific

856   thermal reaction norms in host and pathogen (Jackson & Tinsley, 2002). Whilst some

857   previous studies have emphasized the magnifying effects of warming temperature

858   regimens on host susceptibility in specific systems (Macnab & Barber, 2012), it is

859   also possible to find examples where rising temperature increases

860   resistance (Jackson & Tinsley, 2002; Douglas *et al.*, 2003; Raffel *et al.*, 2013).

861   Furthermore, in other cases infectious disease may show convex responses to

862   temperature, for example with symptoms emerging across a limited temperature

863   range (Gilad *et al.*, 2003; Ito & Maeno, 2014). This can result from non-linear

864   thermal reaction norms in host and or parasite. Thus, although thermal change, all

865   other things being equal, readily shifts the burden of disease caused by individual

866   pathogen species, the direction of these shifts may not be consistent, and the overall

867   disease outcome in host-parasite communities is likely to play out in a system

868   specific way.

869

870   Elements of our results also provide an additional perspective to those of (Dittmar *et*

871   *al.*, 2014) who examined head kidney (HK) cell responses and immune gene

872   expression in *G. aculeatus* under different thermal regimens and with an emphasis

873   on the upper end of the natural temperature range. These authors concluded that

874   high levels of certain HK cellular responses at 13°C corresponded to high

875   immunocompetence and that increased gene expression responses at higher

876   temperatures (correlating negatively with body condition) were indicative of

877   immunopathology and dysregulation. This interpretation for cellular responses is

878   partly consistent with our laboratory results. For example, under our present study

879   conditions, both *Saprolegnia* and *Schistocephalus* disease progression worsened as

880   the temperature rose (all other things being equal), although this could also relate to

881   the cold-biased expression of some innate immune pathways that we observed here.

882   On the other hand, we found that under natural circumstances (in mesocosms) high

883   expression of adaptive immunity genes (such as *ighm*) correlated with high

884   immunocompetence and also coincided with the warmest times of year.

885   Furthermore, in late summer (in the weeks following seasonal peaks in temperature)

886   we have not found fish exposed to natural temperature variation to undergo marked

887   reductions in condition (Hablützel *et al.*, 2016). Rather the genome-wide

888   transcriptomic signatures seen in wild fish at this time of year include adaptive

889   immune activity and also growth and development (Brown *et al.*, 2016), the latter

890   indicative of robust health. Taken together, these observations suggest that, within

891   the normal range of temperatures (although perhaps not at the more extreme

892   temperatures considered by Dittmar *et al.*), high immune gene expression does not

893   necessarily equate to dysregulation and may reflect effective resistance responses.

894   In conclusion, we generated a realistic mid-latitude climatic warming scenario in

895   outdoors mesocosms, incorporating precise temperature control. With this we

896   demonstrated significant perturbation of immunity and infectious disease progression

897   under modest incremental warming (+2°C) in a representative natural model CBV

898   (the three-spined stickleback). These perturbations included changes in both the

899 magnitude and phenology of disease that might be of practical importance in real-

900 world situations. Parallel laboratory experimental analyses confirmed that thermally-

901 driven responses of immunity and infectious disease progression were substantial.

902 When all else was equal, thermal effects were most strongly dependent on the

903 prevailing temperature (the latter, in the case of infection, here taken to encompass

904 temperature regimen post-invasion). Lagged thermal effects (preceding invasion, in

905 the case of infection) were less important. The contrasting responses to thermal

906 manipulation of our different infection systems confirm that increases in temperature

907 can worsen or ameliorate disease progression according to the specific thermal

908 biology of the host and pathogen. Thus, in an otherwise constant warming

909 environment, within-host outcomes would likely to play out in a system-specific way

910 in complex host-parasite communities, without necessarily increasing the overall

911 burden of disease. Most importantly, by combining our mesocosm observations with

912 experimentally-derived estimates of thermal effects, we show that, in a seasonal

913 natural system, thermal effects are superimposed upon substantial temporal

914 variation in immunocompetence. The latter is driven by non-thermal aspects of the

915 environment and, for *Saprolegnia*-mediated disease, its effect is at least as large as

916 that of thermal variation. Critically, thermal change is likely to indirectly affect the

917 non-thermal environmental drivers of immunocompetence, additional to its direct

918 effects on disease progression. Thus, projection of infection dynamics based on

919 experimentally-determined thermal effects alone is unlikely to be reliable, given the

920 size of non-thermal environmental effects on immunocompetence. In practical

921 management situations, the accuracy of such projections might be improved by

922 primarily considering prevailing (and not lagged) thermal effects and by incorporating

923 validated measures of immunocompetence (such as *ighm* expression in the case of

924 *Saprolegnia* here).

References

Abramoff MD, Magalhães PJ, Ram SJ (2004) Image processing with ImageJ. *Biophotonics international,* **11**, 36-42.

Altman KA, Paull SH, Johnson PTJ, Golembieski MN, Stephens JP, Lafonte BE, Raffel TR (2016) Host and parasite thermal acclimation responses depend on the stage of infection. *Journal of Animal Ecology,* **85**, 1014-1024.

Andersen PS, Buchmann K (1998) Temperature dependent population growth of *Gyrodactylus derjavini* on rainbow trout, *Oncorhynchus mykiss. Journal of Helminthology*, **72**, 9-14.

Barber I, Berkhout BW, Ismail Z (2016) Thermal change and the dynamics of multi-host parasite life cycles in aquatic ecosystems. *Integrative and Comparative Biology,* **56**, 561-572.

Barber I, Scharsack JP (2010) The three-spined stickleback-*Schistocephalus solidus* system: an experimental model for investigating host-parasite interactions in fish. *Parasitology,* **137**, 411-424.

Beldomenico PM, Telfer S, Gebert S, Lukomski L, Bennett M, Begon M (2008) The dynamics of health in wild field vole populations: a haematological perspective. *Journal of Animal Ecology*, **77**, 984-997.

Bly JE, Clem LW (1992) Temperature and teleost immune functions. *Fish and Shellfish Immunology,* **2**, 159-171.

Bly JE, Lawson LA, Dale DJ, Szalai AJ, Durburow RM, Clem LW (1992) Winter saprolegniosis in channel catfish. *Diseases of Aquatic Organisms,* **13**, 155-164.

Brown M, Hablützel P, Friberg IM, Thomason AG, Stewart A, Pachebat JA, Jackson JA (2016) Seasonal immunoregulation in a naturally-occurring vertebrate. *BMC Genomics,* **17**, 1-18.

Buehler DM, Piersma T, Matson K, Tieleman BI (2008) Seasonal redistribution of immune function in a migrant shorebird: annual-cycle effects override adjustments to thermal regime. *American Naturalist,* **172**, 783-796.

Dittmar J, Janssen H, Kuske A, Kurtz J, Scharsack JP (2014) Heat and immunity: an experimental heat wave alters immune functions in three-spined sticklebacks (*Gasterosteus aculeatus*). *Journal of Animal Ecology,* **83**, 744-757.

Douglas CW, Ross AA, Gerry M (2003) Emerging disease of amphibians cured by

965   elevated body temperature. *Diseases of Aquatic Organisms,* **55**, 65-67.

966   Fregeneda-Grandes JM, Carbajal-Gonzalez MT, Aller-Gancedo JM (2009)

967   Prevalence of serum antibodies against *Saprolegnia parasitica* in wild and

968   farmed brown trout *Salmo trutta. Diseases of Aquatic Organisms,* **83**, 17-22.

969   Garner TWJ, Rowcliffe JM, Fisher MC (2011) Climate change, chytridiomycosis or

970   condition: an experimental test of amphibian survival. *Global Change Biology,*

971   **17**, 667-675.

972   Gelnar M (1990) Experimental verification of the water temperature effect on the

973   micropopulation growth of *Gyrodactylus rutilensis* Glaser, 1974 (Monogenea).

974   *Folia Parasitologica (Praha),* **37**, 113-114.

975   Gilad O, Yun S, Adkison MA, Way K, Willits NH, Bercovier H, Hedrick RP (2003)

976   Molecular comparison of isolates of an emerging fish pathogen, koi

977   herpesvirus, and the effect of water temperature on mortality of experimentally

978   infected koi. *Journal of General Virology,* **84**, 2661-2667.

979   Hablützel IP, Brown M, Friberg IM, Jackson JA (2016) Changing expression of

980   vertebrate immunity genes in an anthropogenic environment: a controlled

981   experiment. *BMC Evolutionary Biology,* **16**, 1-12.

982   Harris P (1982) Studies of the Gyrodactyloidea (Monogenea). Unpublished Ph. D.

983   University of London.

984   Harris PD, Cable J, Tinsley RC, Lazarus CM (1999) Combined ribosomal DNA and

985   morphological analysis of individual gyrodactylid monogeneans. *Journal of*

986   *Parasitology,* **85**, 188-191.

987   Hatai K, Hoshiai G-I (1993) Characteristics of two *Saprolegnia* species isolated from

988   Coho salmon with saprolegniosis. *Journal of Aquatic Animal Health,* **5**, 115-

989   118.

990   IPCC (2014) Climate Change 2014: Synthesis Report. Contribution of Working

991   Groups I, II and III to the Fifth Assessment Report of the

992   Intergovernmental Panel on Climate Change. Geneva, Switzerland, IPCC.

993   Ito T, Maeno Y (2014) Effects of experimentally induced infections of goldfish

994   *Carassius auratus* with cyprinid herpesvirus 2 (CyHV-2) at various water

995   temperatures. *Diseases of Aquatic Organisms,* **110**, 193-200.

996   Jackson JA, Tinsley RC (1994) Infrapopulation dynamics of *Gyrdicotylus gallieni*

997   (Monogenea: Gyrodactylidae). *Parasitology,* **108**, 447-452.

998   Jackson JA, Tinsley RC (2002) Effects of environmental temperature on the

999   susceptibility of *Xenopus laevis* and *X. wittei* (Anura) to *Protopolystoma*

1000   *xenopodis* (Monogenea). *Parasitology Research,* **88**, 632-638.

1001 Jiang RH, De Bruijn I, Haas BJ *et al.* (2013) Distinctive expansion of potential

1002   virulence genes in the genome of the oomycete fish pathogen *Saprolegnia*

1003   *parasitica*. *PLoS Genetics,* **9**, e1003272.

1004 Karvonen A, Kristjánsson BK, Skúlason S, Lanki M, Rellstab C, Jokela J (2013)

1005   Water temperature, not fish morph, determines parasite infections of

1006   sympatric Icelandic threespine sticklebacks (*Gasterosteus aculeatus*).

1007   *Ecology and Evolution,* **3**, 1507-1517.

1008 Le Morvan C, Troutaud D, Deschaux P (1998) Differential effects of temperature on

1009   specific and nonspecific immune defences in fish. *Journal of Experimental*

1010   *Biology,* **201**, 165-168.

1011 Macnab V, Barber I (2012) Some (worms) like it hot: fish parasites grow faster in

1012   warmer water, and alter host thermal preferences. *Global Change Biology,* **18**,

1013   1540-1548.

1014 Makrinos DL, Bowden TJ (2016) Natural environmental impacts on teleost immune

1015   function. *Fish and Shellfish Immunology,* **53**, 50-57.

1016 Maniero GD, Carey C (1997) Changes in selected aspects of immune function in the

1017   leopard frog, *Rana pipiens*, associated with exposure to cold. *Journal of*

1018   *Comparative Physiology B,* **167**, 256-263.

1019 Martin LB, Weil ZM, Nelson RJ (2008) Seasonal changes in vertebrate immune

1020   activity: mediation by physiological trade-offs. *Philosophical transactions of*

1021   *the Royal Society of London. Series B, Biological Sciences,* **363**, 321-339.

1022 Mignatti A, Boag B, Cattadori IM (2016) Host immunity shapes the impact of climate

1023   changes on the dynamics of parasite infections. *Proceedings of the National*

1024   *Academy of Sciences of the United States of America,* **113**, 2970-2975.

1025 Minor KL, Anderson VL, Davis KS *et al.* (2014) A putative serine protease, SpSsp1,

1026   from *Saprolegnia parasitica* is recognised by sera of rainbow trout,

1027   *Oncorhynchus mykiss*. *Fungal Biology,* **118**, 630-639.

1028 Mori U, Mendiburu A, Lozano JA (2017) Distance measures for time series in R: the

1029   TSdist package. *The R Journal*, **8/2**, 451-459.

1030 Murdock CC, Paaijmans KP, Bell AS, King JG, Hillyer JF, Read AF, Thomas MB

1031   (2012) Complex effects of temperature on mosquito immune function.

1032   *Proceedings of the Royal Society of London. Series B, Biological sciences*,

279, 3357-3366.

O'Reilly CM, Sharma S, Gray DK *et al.* (2015) Rapid and highly variable warming of lake surface waters around the globe. *Geophysical Research Letters,* **42**, 10,773-710,781.

Paull SH, Johnson PTJ (2014) Experimental warming drives a seasonal shift in the timing of host-parasite dynamics with consequences for disease risk. *Ecology Letters,* **17**, 445-453.

Podrabsky JE, Somero GN (2004) Changes in gene expression associated with acclimation to constant temperatures and fluctuating daily temperatures in an annual killifish *Austrofundulus limnaeus*. *Journal of Experimental Biology,* **207**, 2237-2254.

Raffel TR, Halstead NT, Mcmahon TA, Davis AK, Rohr JR (2015) Temperature variability and moisture synergistically interact to exacerbate an epizootic disease. *Proceedings of the Royal Society of London. Series B, Biological Sciences,* **282**, 20142039.

Raffel TR, Rohr JR, Kiesecker JM, Hudson PJ (2006) Negative effects of changing temperature on amphibian immunity under field conditions. *Functional Ecology,* **20**, 819-828.

Raffel TR, Romansic JM, Halstead NT, Mcmahon TA, Venesky MD, Rohr JR (2013) Disease and thermal acclimation in a more variable and unpredictable climate. *Nature Climate Change,* **3**, 146-151.

Rigby RA, Stasinopoulos DM (2005) Generalized additive models for location, scale and shape. *Journal of the Royal Statistical Society: Series C (Applied Statistics),* **54**, 507-554.

Roberts RJ (2012) *Fish Pathology,* Chichester, John Wiley & Sons.

Robertson S, Bradley JE, Maccoll AD (2016) Measuring the immune system of the three-spined stickleback - investigating natural variation by quantifying immune expression in the laboratory and the wild. *Molecular Ecology Resources,* **16**, 701-713.

Scheiner SM (1993) Genetics and evolution of phenotypic plasticity. *Annual Review of Ecology and Systematics*, **24**, 35-68.

Sereno-Uribe AL, Zambrano L, Garcia-Varela M (2012) Reproduction and survival under different water temperatures of *Gyrodactylus mexicanus* (Platyhelminthes: Monogenea), a parasite of *Girardinichthys multiradiatus* in

1067   Central Mexico. *Journal of Parasitology,* **98**, 1105-1108.

1068 Sharma S, Gray DK, Read JS *et al.* (2015) A global database of lake surface

1069   temperatures collected by in situ and satellite methods from 1985-2009.

1070   *Scientific Data,* **2**, 150008.

1071 Shinn AP, Bron JE (2012) Considerations for the use of anti-parasitic drugs in

1072   aquaculture. In: *Infectious disease in aquaculture* (ed. Austin B), pp. 190-217.

1073   Woodhead Publishing Limited, Sawston, Cambridge, UK.

1074 Soetaert K, Petzoldt T (2010) Inverse modelling, sensitivity and Monte Carlo Analysis

1075   in R Using Package FME. *Journal of Statistical Software,* **33**, 28.

1076 Stasinopoulos DM, Rigby RA (2007) Generalized additive models for location scale

1077   and shape (GAMLSS) in R. *Journal of Statistical Software,* **23**, 1-46.

1078 Stolwijk AM, Straatman H, Zielhuis GA (1999) Studying seasonality by using sine

1079   and cosine functions in regression analysis. *Journal of Epidemiology and*

1080   *Community Health,* **53**, 235-238.

1081 Stueland S, Hatai K, Skaar I (2005) Morphological and physiological characteristics

1082   of *Saprolegnia* spp. strains pathogenic to Atlantic salmon, *Salmo salar* L.

1083   *Journal of Fish Diseases,* **28**, 445-453.

1084 Tong YL (1976) Parameter estimation in studying circadian rhythms. *Biometrics,* **32**,

1085   85-94.

1086 Viney ME, Riley EM, Buchanan KL (2005) Optimal immune responses:

1087   immunocompetence revisited. *Trends in Ecology and Evolution,* **20**, 665-669.

1088 Voss Jr EW, Groberg Jr WJ, Fryer JL (1980) Metabolism of coho salmon Ig.

1089   Catabolic rate of coho salmon tetrameric Ig in serum. *Molecular Immunology,*

1090   **17**, 445-452.

1091 Wood SN (2006) *Generalized additive models: an introduction with R,* Boca Raton,

1092   Florida, Chapman & Hall/CRC.

1093 Ye J, Bromage ES, Kaattari SL (2010) The strength of B cell Interaction with antigen

1094   determines the degree of IgM polymerization. *The Journal of Immunology*,

1095   **184**, 844–850.

1096 Ye J, Kaattari IM, Ma C, Kaattari S (2013) The teleost humoral immune response.

1097   *Fish and Shellfish Immunology,* **35**, 1719-1728.

1098 Zimmerman LM, Paitz RT, Vogel LA, Bowden RM (2010) Variation in the seasonal

1099   patterns of innate and adaptive immunity in the red-eared slider (*Trachemys*

1100   *scripta*). *Journal of Experimental Biology,* **213**, 1477-1483.